Research Square

Preprints are preliminary reports that have not undergone peer review.
They should not be considered conclusive, used to inform clinical practice,
or referenced by the media as validated information.

Optimization of Functional Polyols and Performance Modulation for WPU Coating Fabrication

Chao Zheng
Haitao Zhou
yan liu
04120006@sues.edu.cn

Shanghai University of Engineering Science - Songjiang Campus: Shanghai University of Engineering Science https://orcid.org/0000-0002-1880-2664

Wenjie Yin
Wulin Xia
Binjie Xin

Research Article

Keywords: polyol, waterborne polyurethane, hydrophobic, glycerol monostearate, terminal hydroxyl silicone oil

Posted Date: June 25th, 2026

DOI: https://doi.org/10.21203/rs.3.rs-10026891/v1

License: This work is licensed under a Creative Commons Attribution 4.0 International License.
Read Full License

Abstract

In this study, the influence of polyol type and molecular weight on the performance of Waterborne polyurethanes (WPUs) was systematically investigated. WPUs systems modified with long fatty side chains were successfully prepared by innovatively introducing terminal hydroxyl silicone oils to construct a heterostructure and using glycerol monostearate as a functional chain extender. Characterization via FTIR, TGA, SEM, and contact angle testing confirmed that when polytetrahydrofuran ether diol (PTMG) with a molecular weight of 2000 g/mol was selected as the soft segment, the resulting material exhibited significant synergistic effects. Its water contact angle reached 108.7°, and the 72 h water absorption rate was only 10.78% markedly lower than that of WPUs derived from other polyols. Additionally, when the film was heated to 250℃, only 5 wt% decomposed. This material combines excellent hydrophobicity, low water absorption, good thermal stability, and mechanical properties. The significantly enhanced water resistance effectively addresses the application limitations of traditional waterborne coatings in humid environments. It provides a theoretical foundation and process reference for developing high-performance eco-friendly protective coatings, particularly suitable for ship anticorrosion, outdoor building materials, and other harsh weathering applications.

1. Introduction

WPUs are an environmentally friendly polymer material synthesized through the stepwise polymerization reaction of isocyanate and polyol[1, 2]. It exhibits excellent mechanical properties, structural designability, and low volatile organic compound (VOC) emissions[3], making it an indispensable functional material in fields such as automobile manufacturing, biomedicine, and intelligent building materials[4–6]. The core of its performance regulation lies in polyol molecular engineering strategy, the chemical topology of the polyol directly governs the cross-linking density, thermodynamic properties, and functionalization potential of the polyurethane network[7, 8]. Current research and development of functionalized WPUs for high-end applications focus on constructing self-healing, superhydrophobic, and electrically conductive properties[9, 10]. Among these, hydrophobic WPUs hold particularly high strategic value for marine anticorrosion and waterproof coatings[11, 12]. However, significant technological barriers remain in optimizing their performance mechanisms and scaling up their preparation[13].

From the perspective of sustainable chemistry, bio-based polyols (e.g., epoxidized vegetable oils, lignin-derived polyols) are increasingly replacing petroleum-based raw materials due to their renewable nature[14–16]. For instance, Wei et al[17] replaced butanediol with chitosan of different molecular weights as a chain extender for PU. At the same time, the introduction of CS5K-50% chitosan enabled the polyurethane to exhibit excellent mechanical properties and good degradability. However, inherent limitations of biomass feedstocks—such as broad hydroxyl value distribution (restricting crosslinked network formation) and complex purification/modification processes (hindering large-scale production)—typically result in products with lower mechanical strength (hardness and modulus) than petroleum-based systems[18, 19]. In contrast, petroleum-based polyols remain dominant in industrialized high-

performance WPUs production. Their uniform hydroxyl values, mature processing technology, and cost advantages enable precise molecular design for demanding applications like aerospace and electronic encapsulation[20]. Regarding hydrophobic functionalization, traditional fluorination strategies achieve static contact angles > 120°. For example, Zhao et al[21] developed a functional WPUs finishing agent via synergistic organofluorine/organosilicon modification. Leather treated with this SiF-WPUs agent attained a water contact angle of 124.26° while retaining mechanical integrity and softness. Nevertheless, environmental persistence, high synthesis costs, and processing instability impede its industrialization. Consequently, current research focuses on non-fluorinated modification routes[22]. By constructing molecular-level hydrophobic microdomains and leveraging micro-nano hierarchical structures, these approaches maintain eco-friendliness while achieving contact angles exceeding 100°. Dai et al[23] demonstrated this through a green, simple method: spraying textiles with WPUSs coatings containing 80% cellulose nanocrystals (CNC) and 20% graphene. The resulting fabrics exhibited contact angles of 103.4° (polyurethane) and 153.6° (textile coating), alongside exceptional electromagnetic shielding and low reflectivity. This work provides innovative pathways for next-generation green functional coatings[24–26].

In addition, the incorporation of long fatty side-chain alkyl groups into polyurethane molecular chains enables significant regulation of material microstructure and macroscopic properties[27, 28]. On one hand, the hydrophobic nature of long alkyl chains reduces surface energy and increases static water contact angles, while their steric hindrance inhibits water molecule penetration to lower water absorption rates. This collectively imparts excellent water resistance and antifouling properties[29, 30]. On the other hand, alkyl chain crystallization enhances micro-domain ordering within hard segments, improving tensile strength and thermal stability. However, excessive alkyl chain content may restrict chain segment mobility, potentially reducing material flexibility[31, 32].

This study aims to develop an environmentally friendly synthesis route for WPUs dispersions, with the core objective of completely eliminating organic solvents from traditional processes. To systematically investigate the impact of polyols on the final material properties, we designed and prepared a series of polyurethane composites. The key variables were polyol chemical type and molecular weight as soft segment raw materials. To enhance composite performance, we innovatively introduced two functional additives: specific proportions of PDMS and GMS. PDMS incorporation significantly enhances material hydrophobicity, surface lubricity, and low-temperature resistance. GMS primarily functions as an internal lubricant and mold release agent, improving processing performance, reducing film surface tackiness, and potentially modifying microphase separation structures. This synergistic modification strategy targets comprehensive optimization of key polyurethane composite properties, including surface characteristics, processability, thermal stability, and mechanical performance.

2. Experimental

2.1 Materials

Isophorone diisocyanate (IPDI) and 2,2-dihydroxymethylpropionic acid (DMPA) were purchased from Aladdin, polytetrahydrofuran ether (PTMG, Mn = 2000, Mn = 1000), polyethylene glycol (PEG, Mn = 2000, Mn = 1000), polycaprolactone (PCL, Mn = 2000, Mn = 1000) trimethylolpropane (TMP) and catalyst (DY-20) were purchased from Shanghai Titan Technology Co., Ltd, terminal hydroxyl silicone oil (PDMS) was provided by Guangzhou Sloco Polymer Co., Ltd, glycerol monostearate (GMS) was purchased from Wuxi Fengsheng Biotechnology Co., Ltd, triethylamine (TEA), ethylenediamine (EDA), and with acetone (ACE) were from SINO PHARMA CHEMICAL REAUTY CO. Hydroxyethyl methacrylate (HEMA) was donated by Shanghai Zhanchen Coatings Co., Ltd. and the deionized water used for the experiments was prepared in the laboratory.

2.2 Material Pre-treatment

To prevent moisture-isocyanate side reactions from affecting experimental results, all reagents were dried using molecular sieves or a vacuum oven.

2.3 Preparation of WPU

Under nitrogen protection, predetermined molar amounts of various polyols and PDMS were charged into a three-necked flask. Subsequently, IPDI and catalyst DY-20 were added. The reaction mixture was heated to 110°C in an oil bath and pre-polymerized for 3 h with stirring at 300–400 rpm. After cooling to 80°C, vacuum-dried GMS, DMPA, and a measured amount of acetone were added sequentially. The reaction was maintained for 4 h. The temperature was then adjusted to 75°C, and TMP was added to conduct the crosslinking reaction for 2 h. HEMA was subsequently added in batches for end-capping modification. After 2 h, a sample was taken to determine the -NCO content. Upon cooling to 35°C, TEA was added and allowed to react for 30 minutes to achieve neutralization. Finally, deionized water was added as the dispersion medium. The mixture was emulsified for 30 minutes using a high-speed shear emulsifier, yielding a WPUs dispersion with a solid content of 25%. The synthesis mechanism of WPUs is schematically presented in Fig. 1.

WPUs prepared from different kinds of polyols PCL (Mn = 1000, Mn = 2000), PTMG (Mn = 1000, Mn = 2000) and PEG (Mn = 1000, Mn = 2000); named respectively: LWPU-1, LWPU-2, MWPU-1, MWPU-2, EWPU-1, EWPU-2.

2.4 Preparation of WPU Films and Coatings

The glass and PTFE plates were sequentially ultrasonicated in acetone and then ethanol for 15 minutes each, rinsed thoroughly with deionized water, and dried. The synthesized WPUs emulsions were applied onto the plates and left to dry at room temperature for 3 days before being collected for subsequent testing.

2.5 Characterization

2.5.1 WPU Emulsion Appearance and Stability Testing

The WPU dispersions samples were centrifuged (TDL-80-2B, Shanghai Anting Scientific Instrument Factory Co., Ltd., China) at 3000 rpm for 30 min. After centrifugation, the samples were visually inspected for stratification and precipitate precipitation.

2.5.2 Emulsion Particle Size Analysis

Water-based polyurethane dispersion samples were diluted with deionized water to a suitable concentration, and subsequently, the diluted emulsions were transferred to a cuvette and left to stand for 5 min to eliminate air bubbles and temperature fluctuation interference. The particle size distribution of the emulsions was determined using a dynamic light scattering laser particle size analyzer (DLS, Nano-ZS90, Malvern, UK) at a constant temperature of 25℃. The detection angle was set to 90°, and the measurements were repeated independently for three times for each sample, and the volumetric average particle size was calculated automatically, and the final result is the average of the three measurements.

2.5.3 Water Absorption Test

Water absorption of WPUs films was tested using the immersion-weighing method. Standard-sized films (e.g., 10×10×1 mm³) were first dried to constant weight. These samples were then immersed in deionized water at 25℃, removed at designated intervals (1 h, 3 h, 6 h, 12 h, 24 h, and 72 h), and weighed after blotting surface moisture. The water absorption rate was calculated as follows:

$$W = \frac{m_1 - m_0}{m_0} \times 100\%$$

Where m_0 is the initial mass of the film and m_1 is its mass after immersion. This test was designed to systematically evaluate the material's hydrophobicity, network porosity, and cross-linking stability, providing a quantitative basis for assessing modification efficacy.

2.5.4 FTIR Analysis of WPU Films

The prepared WPUs film was vacuum-dried at 50℃ for 24 h to eliminate moisture interference during testing. Specimens (1×1 cm²) were cut and mounted flush against the ATR crystal surface. Constant pressure was maintained during measurements to ensure full sample-probe contact. Three distinct regions per specimen were analyzed independently to account for local compositional heterogeneity.

2.5.5 Thermal Stability Testing of WPU Films

To evaluate the thermal stability of WPUs films at elevated temperatures, thermogravimetric analysis was performed using a TGA-4000 instrument (PerkinElmer Inc., USA). Specimens (6–10 mg) were prepared by cutting the films prior to testing to ensure accurate mass measurement. Experiments were conducted under a nitrogen atmosphere (50 mL/min flow rate) to prevent oxidative degradation. A temperature program from 30℃ to 700℃ at 10℃ /min heating rate was employed, ensuring linear temperature control while balancing thermal decomposition resolution and hysteresis effects. Key thermal stability parameters - including decomposition onset temperature, peak degradation

temperature, and residual mass - were systematically determined by monitoring mass loss as a function of temperature.

2.5.6 Testing of Mechanical Properties of WPU Films

Tensile tests were performed on WPUs films using an electronic universal testing machine (AGS-X 10kN STD, Shimadzu, Japan). Specimens were cast in dumbbell-shaped polytetrafluoroethylene (PTFE) molds with 2 mm depth, yielding standardized samples of 75×12.5×0.2 mm (length×width×thickness). All tests were conducted at a crosshead speed of 100 mm/min.

2.5.7 Static Contact Angle Analysis of WPU Coatings

The prepared WPUs emulsion was uniformly coated onto clean glass substrates and cured in a forced-air oven at 60℃ for 48 h. Water contact angles were measured using an optical tensiometer (SDC-200S, Dongguan Shengding Precision Instrument Co., Ltd., China) with deionized water as the test liquid. For each film, five random locations were tested at 25℃. The average value was calculated after excluding outliers to ensure data reproducibility.

2.5.8 Microstructure Analysis of WPU Films

The treated WPUs film samples were sputter-coated with gold and mounted on the stage of a field emission scanning electron microscope (Hitachi SU-8000, Tokyo, Japan). Multiple regions were imaged to analyze surface roughness and microstructural features. To prevent charging effects, samples received uniform conductive coating prior to imaging. Each experimental condition was replicated three times to verify morphological consistency.

3. Results and Discussion

3.1 Stability Analysis of WPU Emulsions

As shown in Fig. 2(a) and (b), the WPUs emulsion remained a homogeneous milky white after centrifugation at 3000 rpm for 30 min, with no visible precipitation. This demonstrates its excellent physical stability and suggests that the emulsion's stability period is likely not less than 6 months under conventional storage conditions (sealed and stored at 25℃ away from light).

The typical milky-white appearance of the emulsion shown in Fig. 2(a) originates from the Mie scattering of visible light by its nanoscale latex particles. This optical property is closely related to both the particle size and the refractive index of the dispersed phase. Through the introduction of terminal hydroxyl silicone oil during prepolymer synthesis, its hydroxyl groups (-OH) react with isocyanate groups (-NCO) to form chemical bonds, thereby enhancing compatibility between the silicone and the polyurethane matrix. Furthermore, the hydrophobic chain segments of this silicone oil migrate towards the surfaces of the emulsion particles, forming a hydrophobic protective layer. This layer reduces the inter-particle van der Waals forces and consequently the tendency of the particles to aggregate, thus enhancing the mechanical stability. Simultaneously, the inherent flexibility of the silicone lowers the glass Tg of the

latex particles. This reduction in Tg decreases the risk of brittle fracture at low temperatures and enhances the freeze-thaw stability.

As listed in Table 1. This highly stable WPUs dispersion can be stored for at least 6 months under proper conditions, a feature that is of great significance for practical production, transportation, and handling.

Table 1
Stability evaluation and appearance analysis of WPUs emulsions

Sample ID	Emulsion appearance	Centrifugal stability	Stability/Month
LWPUS-1	milky white	No precipitation	≥ 6
LWPUS-2	milky white	No precipitation	≥ 6
MWPUS-1	milky white	No precipitation	≥ 6
MWPUS-2	milky white	No precipitation	≥ 6
EWPUS-1	milky white	No precipitation	≥ 6
EWPUS-2	milky white	No precipitation	≥ 6

3.2 Particle Size of WPUs Emulsion

According to the particle size distribution and average particle size test results in Fig. 3(a) and (b), the particle size of WPUs is significantly influenced by the synergistic effect among soft segment type, molecular weight, and additives.

The study demonstrates that using a low molecular weight soft segment (Mn = 1000) significantly reduces prepolymer viscosity due to shorter chain length. This facilitates rapid diffusion and uniform molecular chain dispersion during emulsification, ultimately yielding a stable emulsion with smaller particle size. Conversely, high molecular weight soft segments (Mn = 2000) increase intermolecular entanglement and expand hydrophobic regions due to prolonged chain segments. This impedes emulsification kinetics, resulting in significantly larger particle sizes. Regarding soft segment type: PEG exhibits strong hydrophilicity from dense ether bonds and terminal hydroxyl groups. During emulsification, it preferentially interacts with the aqueous phase to form a compact hydration layer, effectively inhibiting particle aggregation and yielding the smallest particle size (PEG-1000). PTMG, while also polyether-based, possesses lower ether bond density and lacks hydroxyl groups, resulting in slightly reduced hydrophilicity compared to PEG. This leads to a moderately larger particle size (PTMG-1000). PCL's ester bonds and semi-crystalline molecular chain exacerbate microphase separation between soft and hard segments. This effect is particularly pronounced at Mn = 2000, where distinct crystalline domains form, promoting particle coalescence during dispersion and yielding larger particle sizes. Notably, the hydrophobic additive PDMS enriches particle surfaces through interfacial migration, weakening emulsion stability and increasing particle size. However, introducing the emulsifier GMS counteracts this effect by reducing interfacial tension and creating a steric barrier, significantly

mitigating PDMS's negative impact. Collectively, particle size follows this progression: PEG-1000 < PEG-2000 < PTMG-1000 < PTMG-2000 < PCL-1000 < PCL-2000.

The selection of soft segments and the interaction of GMS and PDMS in the formulation design is an effective way to achieve nanoscale dispersion and high performance of WPUs. The conclusions provide an important theoretical basis for the development of environmentally friendly coatings, adhesives, and other applications.

3.3 FTIR of WPU Films

Fourier Transform Infrared Spectroscopy (FTIR) is a characterization technique used to identify molecular structures and functional groups by measuring a substance's absorption of infrared light. Figure 4 presents the FTIR spectrum of the WPUs film, where characteristic absorption peaks associated with WPUS are clearly observable in the wavenumber range of 4000 – 500 cm^{-1}.

Discernible stretching vibration peaks at approximately 3325 cm^{-1} (N-H), 1720 cm^{-1} (free C = O), and 1250 cm^{-1} (C-O-C) correspond to the key characteristic peaks of the carbamate hard segment (-NHCOO-). This confirms the successful reaction between the isocyanate group (-NCO) and polyol or chain extender. Furthermore, the absence of the characteristic peak for the isocyanate group (-NCO) near 2270 cm^{-1} indicates complete consumption of the isocyanate monomer during the reaction, demonstrating good control over the synthesis process. The pronounced C = O stretching vibration peak at 1720 cm^{-1} suggests that the carbonyl groups within the carbamate hard segments are predominantly in a free state. This implies weak hydrogen bonding between the hard segments, likely attributable to their lower proportion and inhibited aggregation. Notably, a high proportion of free carbonyl groups typically correlates with lower tensile strength, higher elongation at break, and enhanced material flexibility. A significant absorption peak near 800 cm^{-1} corresponds to the symmetric stretching vibration of the Si-C bond in the silicone modifier, confirming that PDMS chain segments have been successfully incorporated into the WPUS network via chemical bonding.

Concurrently, a distinct C = C double bond stretching vibration peak at 1630 cm^{-1} indicates that the capping reaction with HEMA partially preserved the photoactive double bonds, providing cross-linkable sites for subsequent UV curing. The introduction of PDMS enhances the coating's static contact angle through its low-surface-energy Si-CH_3 groups. Additionally, the flexible siloxane chain segments of PDMS contribute to inhibiting microcrack propagation. Simultaneously, the CH_3 groups introduced via HEMA synergize with PDMS to realize an integrated hydrophobic-mechanical-functional design for the WPUs.

The FTIR results reveal the regulation mechanism of multi-scale structures in WPUs at the molecular level. This finding provides a key basis for subsequent performance optimization.

3.4 Microscopic Morphology of WPU Films

The surface microscopic morphology of the WPUS film, as shown in Fig. 5 captured by scanning electron microscopy (SEM), reveals clear changes in the microstructures.

The SEM micrographs in Fig. 5 reveal the distinct micromorphological evolution patterns of the three polyurethane film types:(a-b) LWPUs Film: The surface exhibits a continuous, dense morphology overall, devoid of significant macro-defects such as cracks, holes, or particle agglomerations. This suggests a good preparation process, resulting in a structurally homogeneous and intact film surface. (c-d) MWPUs Films: These films show good continuity but exhibit slight surface undulations or folds. This morphology may arise from crystallization or volume contraction of soft segments during phase separation. Specifically: The long-chain PTMG soft segments in MWPU-2 are more prone to orderly chain arrangement, forming local crystalline zones.

This crystallization process, accompanied by volume contraction, leads to surface wrinkling and folding. In contrast, the short-chain PTMG soft segments in MWPU-1 possess lower mobility and weaker crystallization ability, resulting in a smoother surface. (e-f) EWPU Film: This film displays more pronounced holes. These defects are likely related to the strong hydrophilicity of PEG, which increases emulsion viscosity. During film formation, entrained air bubbles become difficult to eliminate, increasing the propensity for bubble-induced holes. This porosity consequently compromises the film's water resistance and hydrophobicity.

3.5 Mechanical Properties of WPU Membranes

The mechanical properties of the water-based polyurethane film, determined by tensile tests using an electronic universal testing machine, are shown in Fig. 6 and Table 2.

PTMG soft segments (Mn = 1000/2000) exhibit optimal comprehensive performance, combining high strength and high elongation at break. This results from flexible ether bonds promoting segmental motion, ordered methylene chains enhancing microphase separation, and synergistic effects between stress-induced crystallization and hard-segment physical crosslinking. PCL soft segments show moderate strength due to ester group polarity and crystallinity, but exhibit significantly reduced elongation due to restricted molecular chain mobility. PEG soft segments achieve high elongation through flexible ether bonds, but strong hydrophilicity severely disrupts microphase separation.

This markedly weakens intermolecular forces, resulting in the lowest strength among the systems. The underlying mechanism resides in the soft segment chemical structure, which governs microphase separation efficiency and segmental mobility, thereby determining the strength-elongation balance. Furthermore, soft segment molecular weight influences polyurethane film mechanical properties differently depending on segment type: PCL-based polyurethane: Increasing molecular weight from 1000 to 2000 slightly increases tensile strength but sharply decreases elongation at break. This occurs because higher molecular weight PCL significantly increases crystallinity, strengthening the physical crosslinking network while severely restricting chain mobility. PTMG-based polyurethane: Higher molecular weight slightly enhances strength while maintaining stable elongation. Flexible ether bonds

preserve segmental mobility, and increased molecular weight only modestly enhances chain entanglement/stress crystallization without compromising deformation capability. PEG-based polyurethane: Increased molecular weight decreases strength while sharply increasing elongation at break. Longer chains exacerbate microphase separation disruption, while enhanced chain flexibility, entanglement effects, and water absorption-induced plasticization synergistically improve extensibility.

The introduction of PDMS and GMS as modifiers is expected to significantly alter the tensile properties of water-based polyurethane films. Both modifiers substantially increase the material's elongation at break: their ultra-flexible segments enhance polymer elastic deformation. However, PDMS addition inevitably causes a marked reduction in tensile strength, primarily due to two factors: PDMS exhibits extremely low compatibility with conventional polyurethane hard segments, severely disrupting the continuity and integrity of the original hard-segment microdomains and weakening the critical physical crosslinking network. PDMS itself possesses very low strength and cannot effectively bear stress. Additionally, PDMS inhibits crystallization within crystalline soft segments and significantly increases the material's overall hydrophobicity. In contrast, GMS—a molecule containing long-chain alkyl groups—also increases elongation at break. This effect stems primarily from its long alkyl chains acting as an "internal lubricant", reducing intermolecular friction and facilitating segmental movement. Its branched structure may also disrupt the ordered arrangement or crystallization of soft/hard segments, further facilitating deformation. However, GMS is similarly expected to reduce tensile strength. While both modifiers enhance elongation, PDMS exerts a stronger softening effect and causes greater strength loss. GMS combines internal lubrication with potential network-weakening effects. Beyond modifying mechanical properties, both modifiers aim to improve the material's hydrophobicity.

Table 2
Tensile properties of GWPUS film

Sample ID	Tensile strength (MPa)	Elongation at break (%)
LWPUS-1	1.41	153.50
LWPUS-2	1.61	161.12
MWPUS-1	2.09	307.28
MWPUS-2	2.21	305.47
EWPUS-1	0.99	250.11
EWPUS-2	0.81	324.10

3.6 Thermal Stability Analysis of WPU Films

TG analysis is a technique used to evaluate the decomposition and mass loss of polymers at elevated temperatures. Figure 7(a) and (b) present the TG and DTG curves of the WPUs films, while Table 3 details specific data from their thermal decomposition process.

Generally, the thermal decomposition of WPUs films occurs in three primary stages: Stage 1 (30–300℃): Mass loss observed between 30–150℃ is attributed to the physical desorption and gradual vaporization of water and residual solvent (acetone) as temperature increases. Thermal decomposition behavior in the 150–300℃ range is dominated by the degradation of soft segments (e.g., PCL, PTMG, PEG): Polyester-type PCL decomposes primarily between 200–280℃, generating caprolactone monomers and gaseous products through ester bond cleavage. Polyether-type PTMG releases small molecules like tetrahydrofuran due to ether bond oxidation between 220–300℃. Hydrophilic PEG, influenced by hygroscopicity, undergoes significant degradation at lower temperatures. Increasing the soft segment molecular weight elevates the peak decomposition temperature by 10–15℃. Stage 2 (300–400℃): Within this temperature range, decomposition is primarily driven by cleavage of the urethane hard segments (-NHCOO-). These segments decompose thermally to release primary amines, carbon dioxide, and olefins. The decomposition temperature is concurrently influenced by hydrogen bond density, crosslinker type, and isocyanate chemistry. Stage 3 (400–700℃): Decomposition involves the deep oxidation and carbonization of residual carbon. The cross-linking agent TMP inhibits thermal oxygen diffusion and slows carbon skeleton decomposition through its three-dimensional cross-linked network. The Si-O-Si chains of PDMS cleave at high temperatures, generating a protective SiO_2 ceramic layer that covers the carbon surface and impedes oxygen infiltration. Mass loss in this stage stems from the oxidation of residual hard segments (producing CO/CO_2) and partial gasification of the carbon layer. The heat-resistant properties of PDMS significantly suppress the secondary mass loss peak typically observed at 400–500℃. The TMP cross-linked network enhances the continuity of the residual carbon by reducing microcrack formation.

The synergistic modification provided by both PDMS and TMP endows the WPUS with excellent flame retardancy and high-temperature dimensional stability. This provides a thermodynamic basis for its potential application in aerospace thermal insulation coatings or flame-retardant composites.

Table 3
TG data analysis of WPUs films

Sample ID	5 wt% weight loss temperature (℃)	10 wt% weight loss temperature (℃)	Maximum weight loss temperature (℃)
LWPUS-1	250.02	279.15	603.93
LWPUS-2	257.55	283.92	613.68
MWPUS-1	256.66	285.75	684.85
MWPUS-2	258.57	294.18	684.89
EWPUS-1	256.34	278.06	685.40
EWPUS-2	255.42	287.93	685.07

3.7 Static Contact Angle Analysis of WPU Coatings

The WCA of WPUs films is a key parameter for evaluating water resistance, governed primarily by the films' internal chemical structure and surface morphology. Figure 8 presents the WCAs measured for the synthesized WPUs series.

The WCA for different formulations of WPUs were measured as follows: LWPUS-1: 103.11°, LWPUS-2: 98.21°, MWPUS-1: 103.58°, MWPUS-2: 108.21°, EWPUS-1: 98.57°, EWPUS-2: 95.21°. Comparative analysis of the WPUS series constructed using three soft segments—PCL, PTMG, and PEG—revealed that the synergistic effect of 30 wt% PDMS and 4 wt% GMS significantly enhanced coating hydrophobicity. This enhancement was attributed to the low-surface-energy properties of PDMS and its role in interfacial modulation. However, differences in the chemical properties and molecular weights of the soft segments also profoundly influenced coating hydrophobicity. This influence occurred through their modulation of phase separation behavior, compatibility between soft and hard segments, and the resulting surface chemical composition. The PTMG-based materials (MWPU series) exhibited a unique positive molecular weight effect: the WCA increased from 103.58° (MWPU-1, PTMG-1000) to 108.21° (MWPU-2, PTMG-2000) as the PTMG molecular weight increased. This phenomenon arises because the polarity contribution of the ether bonds within the PTMG soft segment decreases with increasing molecular weight. Concurrently, the longer PTMG chain structure reduces the polarity difference between the soft segment and PDMS. These factors collectively promote the migration and enrichment of PDMS towards the coating surface, thereby increasing the surface density of $-CH_3$ groups and facilitating the formation of a continuous low-surface-energy layer. In contrast, PCL-based materials (LWPU series) displayed a negative molecular weight effect, with WCA decreasing as PCL molecular weight increased (PCL-1000: 103.11°; PCL-2000: 98.21°). Although PCL itself exhibits strong hydrophobicity due to the high chemical stability of its ester groups and low ether bond content, increasing the soft segment chain length enhances its compatibility with the hard segment. This enhanced compatibility subsequently inhibits the phase migration ability of PDMS. The PEG-based materials (EWPUS series) demonstrated the poorest hydrophobicity (WCA = 95.21° for EWPU-2). The inherent hydrophilicity of the PEG soft segment, stemming from its high density of ether bonds and terminal hydroxyl groups, fundamentally conflicts with the hydrophobicity of PDMS. While the use of GMS emulsification improved dispersion, increasing the PEG molecular weight exacerbated the interfacial incompatibility. Evidence for this includes the broadening of the characteristic Si-O-Si FTIR peak at ~ 1010 cm^{-1}, indicating localized PDMS agglomeration. Furthermore, SEM revealed the presence of micron-sized pores on the surface of the PEG-2000 samples (EWPU-2), providing preferential pathways for water penetration. This combination of structural defects and inherent chemical polarity led to a significant deterioration in the water resistance of the EWPU series. Comprehensive performance comparisons indicate that the PTMG-2000-based WPUS (MWPU-2) is the optimal system, achieving a WCA of 108.21°and withstanding 72h of water immersion without wrinkling. This system shows significant potential for applications in flexible electronic packaging and marine antifouling coatings.

3.8 Water Resistance Testing of WPU Films

The water absorption of WPUs is primarily governed by the chemical polarity of the soft segments, their molecular weight, and the synergistic effects of additives. The water absorption behavior of WPUs synthesized using an IPDI hard segment, combined with different soft segments—PCL, PTMG, and PEG—at molecular weights (M_n) of 1000 and 2000, and modified with 30 wt% PDMS and 4 wt% GMS, is presented in Fig. 9.

PCL-based materials exhibited the lowest water absorption, attributable to their hydrophobic ester groups and crystalline structure. PTMG-based materials, characterized by the moderate hydrophilicity of their ether bonds, showed intermediate water absorption. Conversely, PEG-based materials, possessing strongly hydrophilic ether bonds and hydroxyl groups, demonstrated the highest water absorption. Regarding molecular weight effects, lower molecular weight materials (e.g., PCL-1000) generally displayed lower water absorption due to tighter chain segment stacking and higher crystallinity. Higher molecular weight counterparts (e.g., PCL-2000) exhibited slightly increased water absorption, resulting from enhanced chain flexibility and reduced crystallinity. However, for PTMG-2000, the increased number of ether bonds and consequent strengthening of hydrogen bonding with water led to a reversal of this trend, causing its water absorption to exceed that of the lower molecular weight PTMG. The synergistic effect of PDMS and GMS significantly enhanced overall hydrophobicity: PDMS formed a barrier inhibiting water penetration through surface-enriched hydrophobic methyl groups, while GMS optimized PDMS dispersion, reduced agglomerations, and enhanced coating uniformity. Nevertheless, this improvement proved limited for strongly hydrophilic PEG-based WPUSs, where hydrophilic groups continued to dominate surface properties. Optimization strategies include: Prioritizing PCL or PTMG soft segments, Controlling molecular weight, Increasing PDMS content to 35% and introducing cross-linkers or nanofillers (e.g., SiO_2) to construct a multistage hydrophobic structure, Optimizing the coating process to minimize surface defects. Future work should involve conducting dynamic water absorption experiments combined with microscopic characterization (e.g., using DSC to measure crystallinity and AFM to observe phase separation). This will further quantify the effects of various factors and provide a precise quantitative design basis for applying water-repellent coatings in fields like marine anticorrosion and medical materials.

4. Conclusions

In this study, a series of high-performance WPUs were synthesized using polyol soft segments—PCL, PTMG, and PEG (molecular weights: 1000 or 2000)—combined with GMS and PDMS modification. The results demonstrate that: All WPUs emulsions exhibited particle sizes below 200 nm and resisted delamination under high-speed centrifugation, indicating excellent kinetic stability. GMS further enhanced dispersion homogeneity and long-term storage stability by reducing interfacial tension. The films displayed good thermal stability, with initial decomposition temperatures (T5wt%) exceeding 250°C and maximum decomposition temperatures (Tmax) concentrated between 600°C and 700°C. Regarding water resistance, PEG-based WPUSs exhibited strong hydrophilicity, resulting in a 24h water absorption rate exceeding 40%. In contrast, PTMG-based WPUs demonstrated excellent water resistance due to their hydrophobic soft-segment structure, achieving a water absorption rate below 15% and a water

contact angle greater than 108°. Collectively, PTMG-based WPUSs demonstrate significant potential for applications requiring a combination of high strength, high toughness, outstanding water resistance, and tunable thermal stability. Coupled with the GMS/PDMS molecular design strategy, they provide an effective pathway for developing high-performance, environmentally friendly polyurethane materials.

Declarations

CRediT authorship contribution statement

The manuscript was completed by the first author. All authors reviewed the manuscript.

Declaration of competing interest

The authors declare no conflict of interest.

Data Availability Statement

The authors confirm that the data supporting the findings of this study are available within the article. And no new data were created.

Acknowledgement

No funding was received for conducting this study.

Corresponding Authors

Yan Liu - College of Chemistry and Chemical Engineering, Shanghai University of Engineering Science, Shanghai 201620, China; 0000-0002-1880-2664 Email: 04120006@sues.edu.cn

Binjie Xin - School of Textiles and Fashion Engineering, Shanghai University of Engineering Science, Shanghai 201620, China; orcid.org/0000-0003-0683-8018; Email: xinbj@sues.edu.cn

Authors

Chao Zheng - College of Chemistry and Chemical Engineering, Shanghai University of Engineering Science, Shanghai 201620, China

Haitao Zhou - College of Chemistry and Chemical Engineering, Shanghai University of Engineering Science, Shanghai 201620, China

Wenjie Yin - College of Chemistry and Chemical Engineering, Shanghai University of Engineering Science, Shanghai 201620, China

Wulin Xia - College of Chemistry and Chemical Engineering, Shanghai University of Engineering Science, Shanghai 201620, China

References

1. Xiong W, Chen B, Peng J et al (2024) A dual-crosslinking strategy for waterborne polyurethane coatings to achieve outstanding anti-smudge and anti-corrosion properties. Chem Eng J 490:151509
2. Li Y, Jin Y, Chen H et al (2025) A Visible Light-Responsive, Fast Room-Temperature Self- Healing, Mechanically Robust, Antibacterial Waterborne Polyurethane Based on Triple Dynamic Bonds. ACS Appl Mater Interfaces 17:20307–20323
3. Tan J, Li F, Chen H et al (2025) Amine resin-crosslinked waterborne polyurethane with excellent mechanical properties and water resistance for automotive middle coating. Prog Org Coat 200:109071
4. Han J, Zhu X, Tian L et al (2025) Bio-based waterborne polyurethanes from castor oil, sorbitan monooleate and sodium lignosulfonate with ultraviolet resistance, photothermal effect, corrosion protection and degradation properties. Int J Biol Macromol 287:138471
5. Zhang J, Zhai R, Kang W et al (2025) Construction of waterborne polyurethane crosslinking network with excellent adhesion strength, mechanical properties, and wear resistance. Mater Today Commun 44:112062
6. Lei L, Wang H, Jia Q et al (2023) Highly stretchable, supersensitive, and self-adhesive ionohydrogels using waterborne polyurethane micelles as cross-linkers for wireless strain sensors. J Mater Chem B 11:7478–7489
7. Zhang Z, Han X, Jia L et al (2024) Highly water-resistant transparent waterborne polyurethane thermal-insulation coating material with multiple self-crosslinking network based on controllably activated end-capping reagent. Prog Org Coat 187:108104
8. Zuo Y, Rao Z, Lu W et al (2024) Migration of polydimethylsiloxane chain segments toward the surface of UV-cured waterborne poly(urethane-acrylate) films. Prog Org Coat 192:108504
9. Zhou W, Gong X, Li Y et al (2021) Waterborne electrospinning of fluorine-free stretchable nanofiber membranes with waterproof and breathable capabilities for protective textiles. J Colloid Interface Sci 602:105–114
10. Gu B, Song H, Jiang X et al (2025) Multifunctional bionic hydrophobic cotton fabrics modified with cationic nano-SiO2/polyurethane acrylate. Prog Org Coat 198:108912
11. Kim M-G, Jo K-I, Kim E et al (2021) Preparation of Polydimethylsiloxane-Modified Waterborne Polyurethane Coatings for Marine Applications. Polymers 13:4283
12. Ma Y, Zhang M, Du W et al (2023) Preparation and Properties of Hydrophobic Polyurethane Based on Silane Modification. Polymers 15:1759
13. Zhu X, Zhou C, Pan Z et al (2024) Multifunctional Waterborne Polyurethane with Robustness, Adhesiveness, and Self-Healability Based on a Dual Cross-Linked Network Containing Multiple Dynamic Bonds. ACS Appl Polym Mater 6:13389–13400

14. Lai Y, Qian Y, Yang D et al (2021) Preparation and performance of lignin-based waterborne polyurethane emulsion. Ind Crops Prod 170:113739
15. Gaddam SK, Arukula R (2022) Renewable soft segment-induced anionic waterborne polyurethane dispersions with enriched bio-content. J Polym Res 29:59
16. Zhang Y, Zhang W, Deng J et al (2024) Synthesis of waste soybean oil-based waterborne polyurethane for exploration of its green and various application. Ind Crops Prod 216:118733
17. Wei C-T, You J-L, Chin K-Y et al (2025) Synthesis and characterization of eco-friendly chitosan-based waterborne polyurethanes and their ultraviolet degradation properties. Polym Degrad Stab 233:111169
18. Jang S, Go EM, Kim J-K et al (2022) Optically transparent, ultra-tough, aerosol-sprayable, waterborne polyurethane composite reinforced with natural polymer nanofibers. Compos Part B: Eng 247:110353
19. Xing Y, Li X, Xu J, Zhang F (2024) Organosilicon-modified double crosslinked waterborne polyurethane coatings. Prog Org Coat 190:108372
20. Qiu J, Zhao H, Luan S et al (2025) Recent advances in functional polyurethane elastomers: from structural design to biomedical applications. Biomater Sci 13:2526–2540
21. Zhao W, Sui Z, Zhang Q et al (2024) Waterborne polyurethane containing fluorosilicone coating: to endow leather with enduring hydrophobicity and mechanical properties. Text Res J 94:1924–1935
22. Valčić MD, Cakić SM, Ristić IS et al (2021) Polycaprolactone-based biodegradable acrylated polyurethanes: Influence of nanosilica amount on functional properties. Int J Adhes Adhes 104:102738
23. Dai M, Zhai Y, Zhang Y (2021) A green approach to preparing hydrophobic, electrically conductive textiles based on waterborne polyurethane for electromagnetic interference shielding with low reflectivity. Chem Eng J 421:127749
24. Zhou H, Liu Y, Lu T et al (2025) Novel waterborne polyurethanes extended by glycerol monostearate: their synthesis and application to water repellency. J Polym Res 32:30
25. Lu T, Qin Y, Liu Y et al (2024) Preparation and Properties of Acrylic Acid-Modified Multicross-Linked Two-Component Waterborne Phase-Change Polyurethane. ACS Appl Polym Mater 6:8866–8875
26. Delavarde A, Savin G, Derkenne P et al (2024) Sustainable polyurethanes: toward new cutting-edge opportunities. Prog Polym Sci 151:101805
27. Li J, Zhao L, Hong C et al (2024) Synthesis and characterization of waterborne polyurethane-based ink binder modified via a silane coupling agent. Prog Org Coat 186:108018
28. Zhao M, Yang M, Omoniyi AO et al (2023) Synthesis and performance of hydroxyl-terminated polysiloxane-modified polyurethane acrylate films as potential flexible hydrophobic materials. J Appl Polym Sci 140:e54272
29. Li C, Dong Y, Yuan X et al (2024) Waterborne polyurethane sizing agent with excellent water resistance and thermal stability for improving the interfacial performance of carbon fibers/epoxy

resin composites. Colloids Surf A 681:132817

30. Zhang J, Zhai R, Zhang J et al (2024) Waterborne polyurethane based on dual crosslinked structure with excellent mechanical properties, water and corrosion resistance. Prog Org Coat 197:108784
31. Mao T, Feng H, Wu J et al (2023) Waterborne organic silicone polyurethane with excellent self-healing performance for oil/water-separation and oil-recovery applications. Sustainable Mater Technol 36:e00631
32. Dong H, Wang L, Zhang S et al (2024) Ultra-tough, strong and transparent bio-based waterborne polyurethanes with exceptional anti-corrosion properties. Polymer 315:127802

Figures

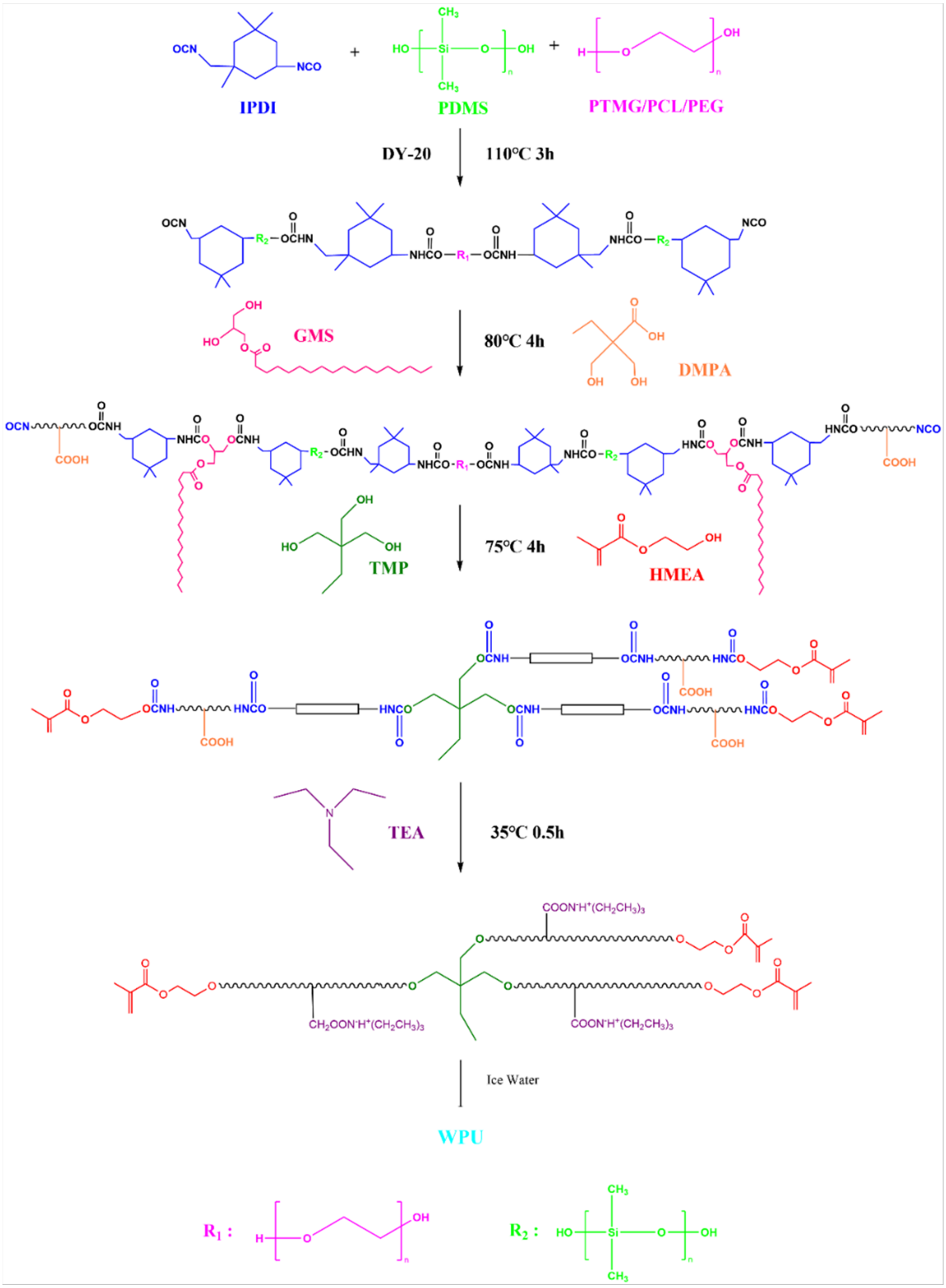


Figure 1

WPUs synthesis mechanism

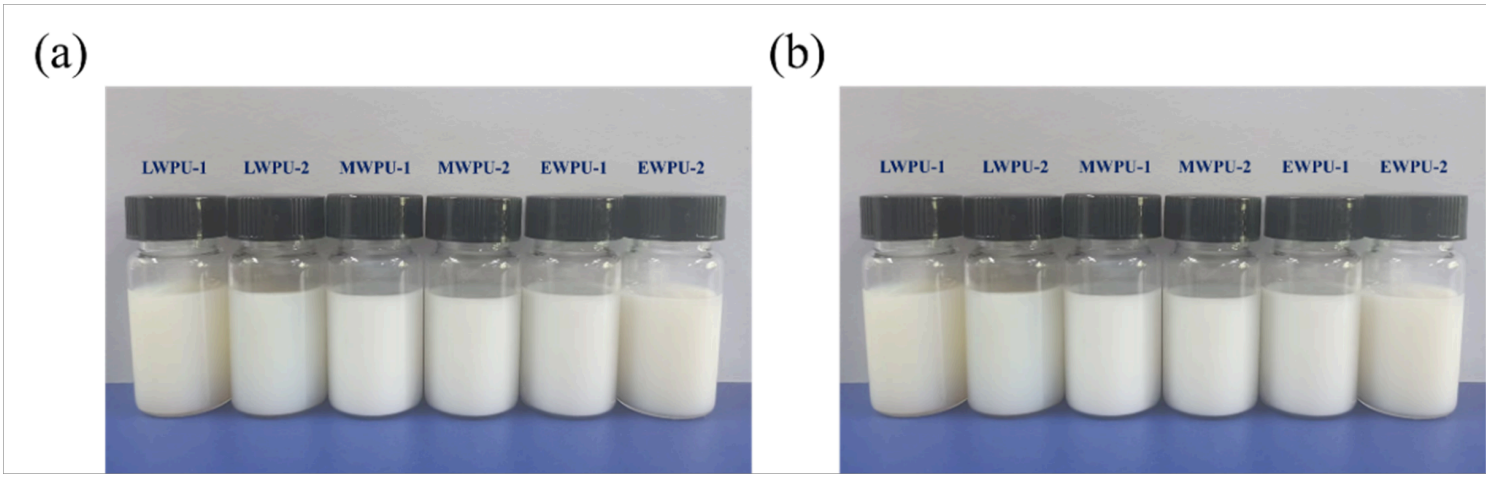


Figure 2

(a) Appearance of WPUs emulsion before centrifugation; (b) Appearance of WPUs emulsion after centrifugation

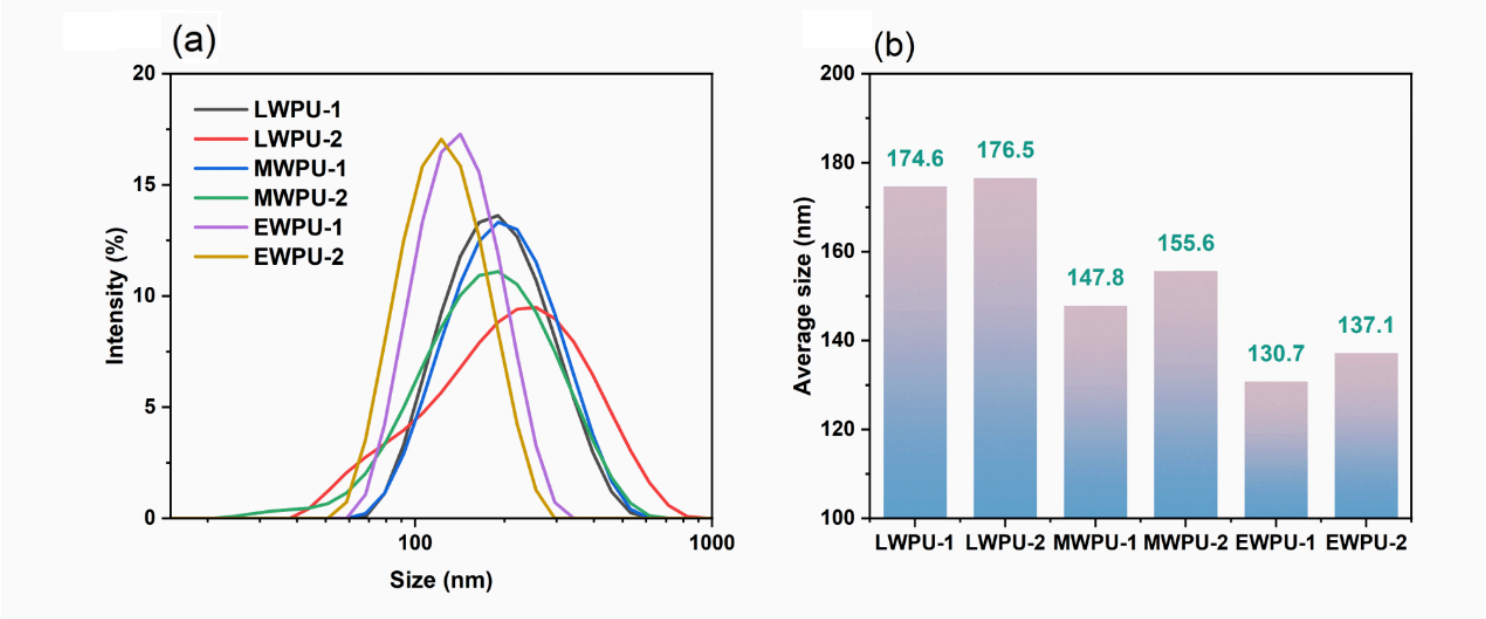


Figure 3

(a) Particle size distribution of WPUs: (b) Mean particle size of WPUs

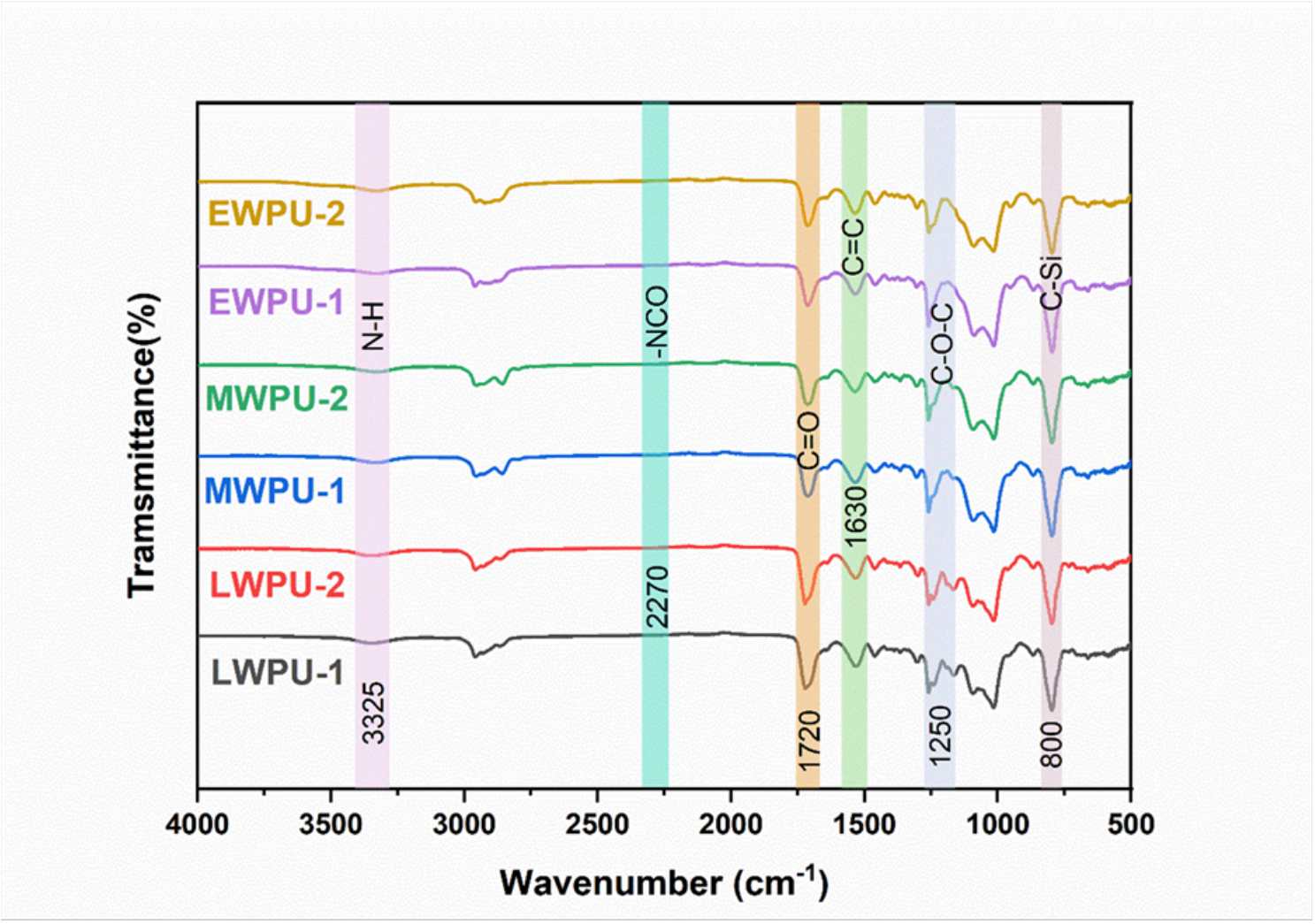


Figure 4

FTIR spectra of WPUs films

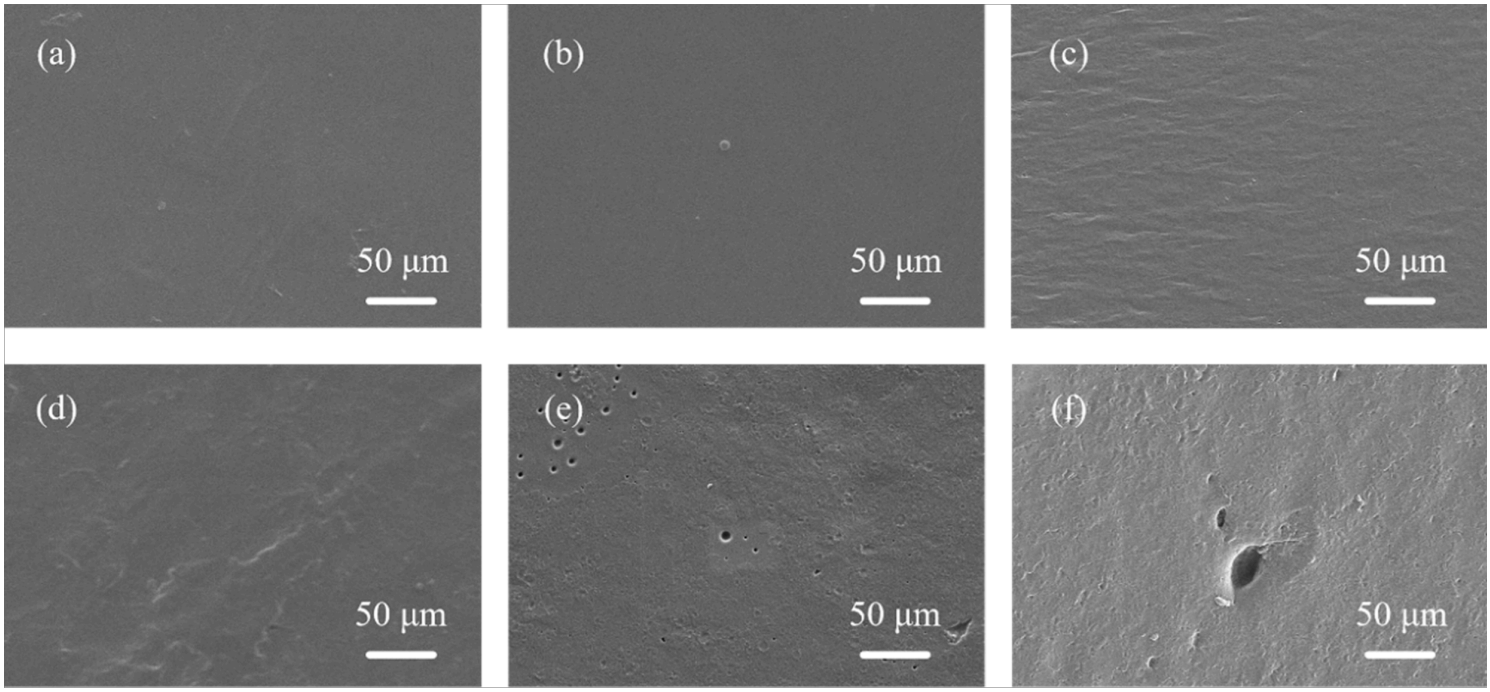


Figure 5

SEM images of WPUS film surfaces: (a) LWPU-1, (b) LWPU-2, (c) MWPU-1, (d) MWPU-2, (e) EWPU-1, (f) EWPU-2

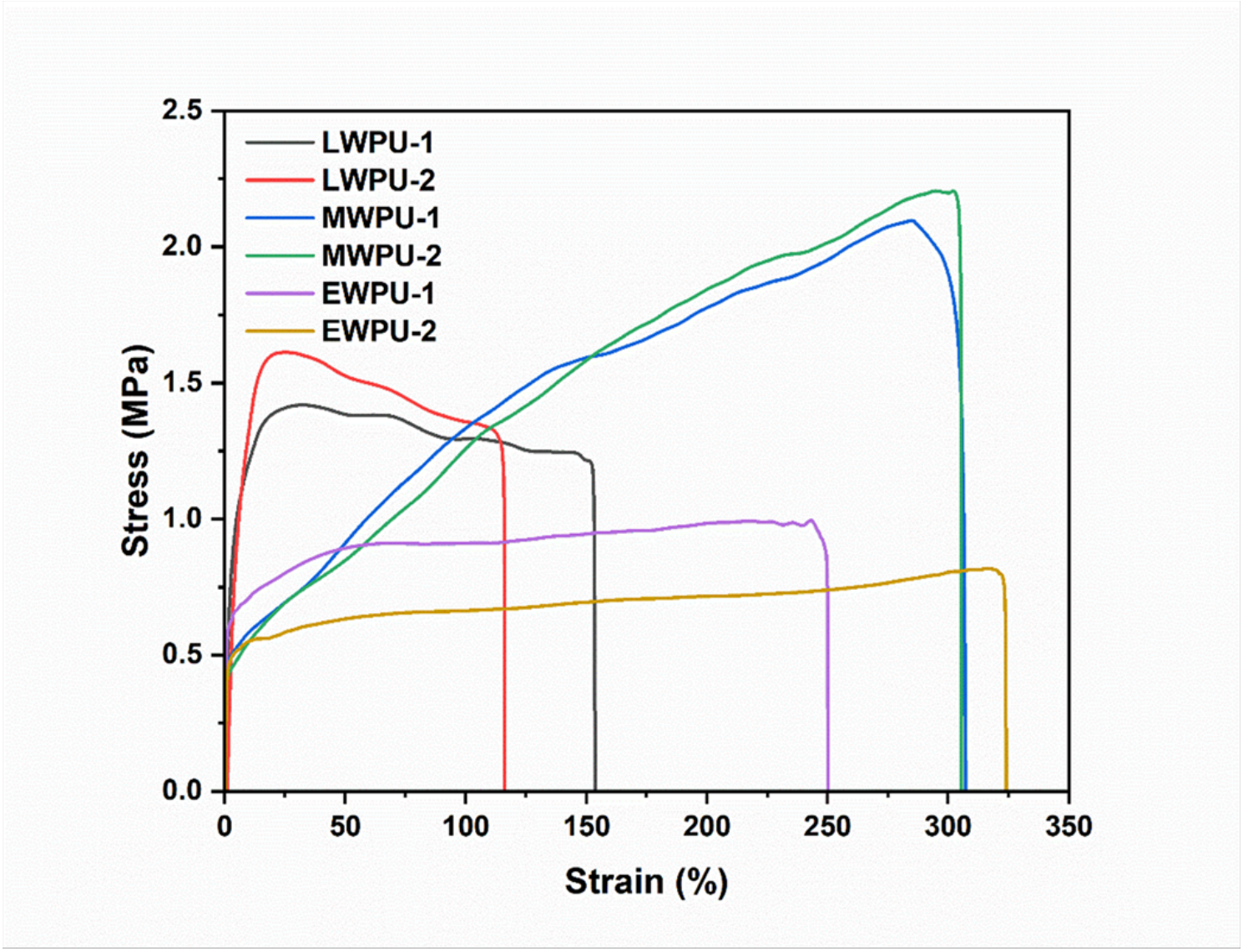


Figure 6

Stress-strain curve of WPUS film

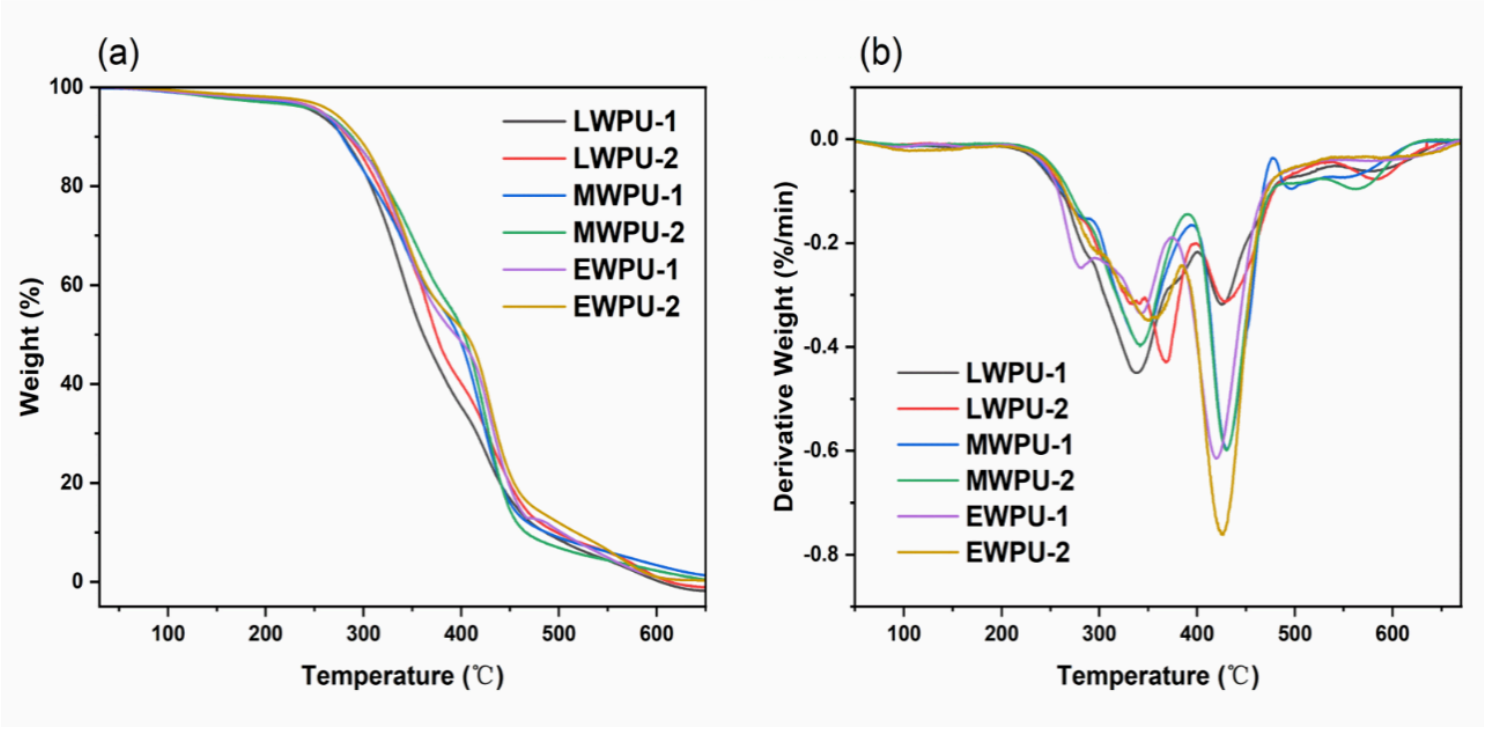


Figure 7

Thermal properties of WPUS: (a) TG curve of WPUS film; (b) DTG curve of WPUs film

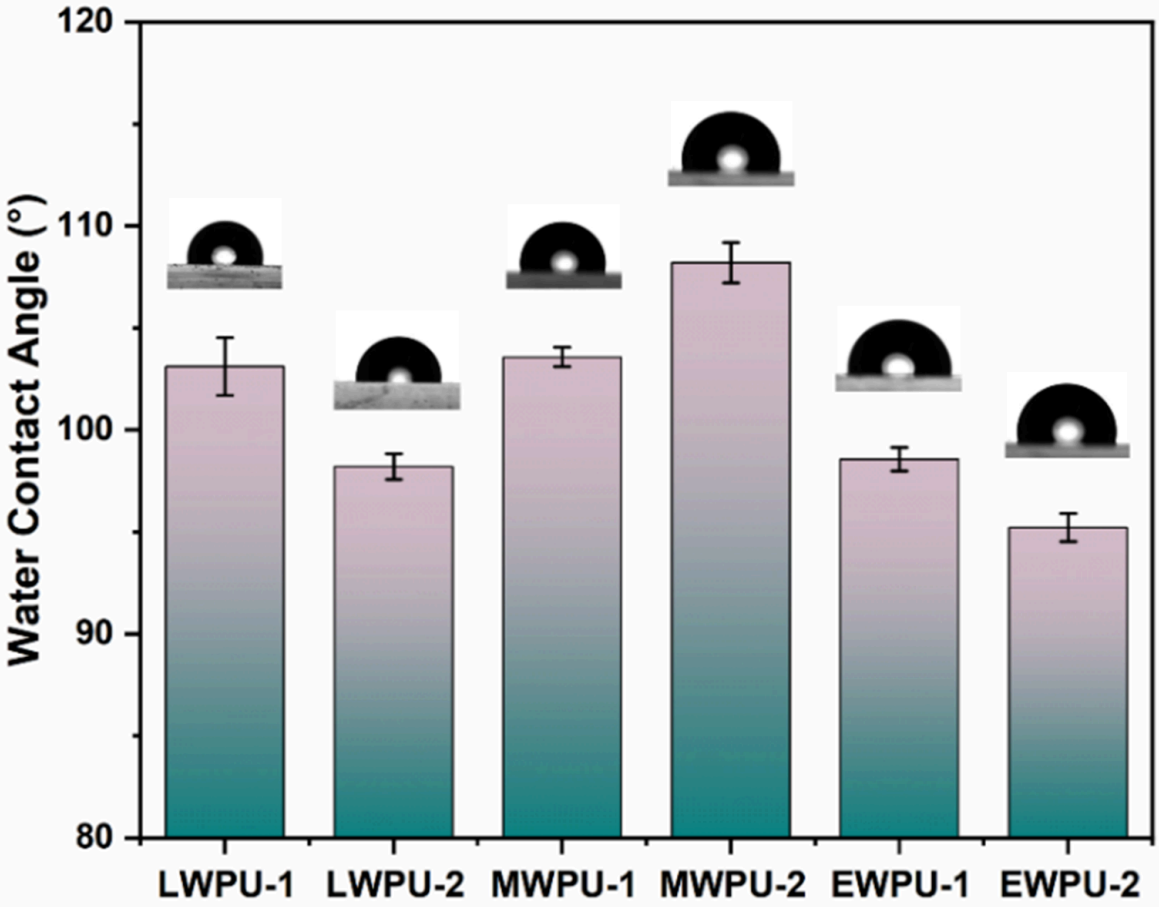


Figure 8

Water contact angle of WPUs film

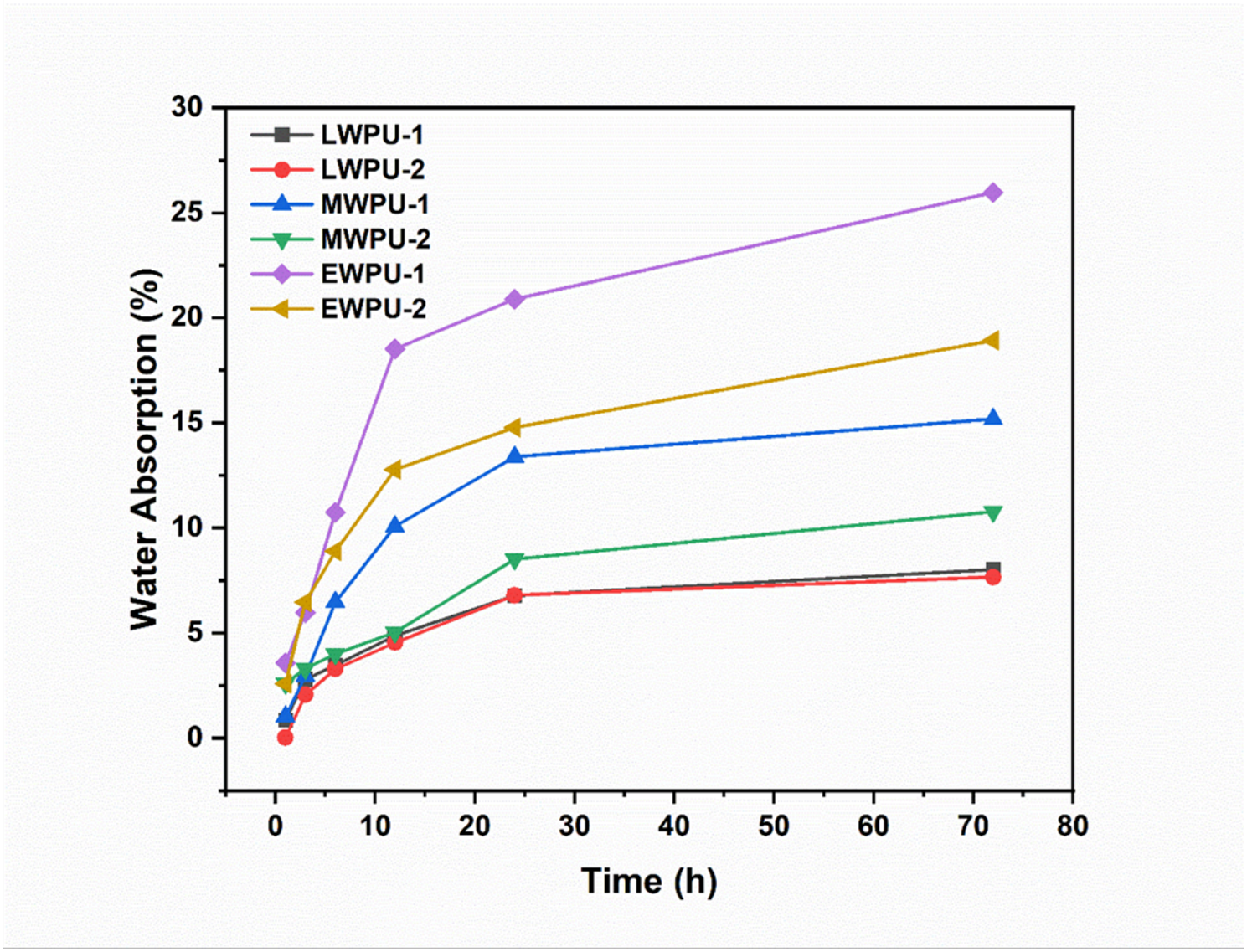


Figure 9

Water absorption of WPUs film